



# Performance of a large-size RPC equipped with the final ATLAS front-end electronics at X5-GIF irradiation facility

G. Aielli<sup>a</sup>, P. Camarri<sup>a</sup>, R. Cardarelli<sup>a</sup>, V. Chiostrì<sup>a</sup>, R. De Asmundis<sup>b</sup>,  
A. Di Ciaccio<sup>a</sup>, L. Di Stante<sup>a</sup>, V. Koreshev<sup>c</sup>, B. Liberti<sup>a,\*</sup>, A. Paoloni<sup>a</sup>,  
E. Pastori<sup>a</sup>, R. Perrino<sup>d</sup>, R. Santonico<sup>a</sup>, V. Zaets<sup>c</sup>

<sup>a</sup>*Dipartimento di Fisica, Università di Roma "Tor Vergata", and I.N.F.N.- Sezione di Roma 2, Via della Ricerca Scientifica, 1-00133 Roma, Italy*

<sup>b</sup>*Dipartimento di Fisica, Università di Napoli and I.N.F.N. - Sezione di Napoli, Italy*

<sup>c</sup>*Institute for High Energy Physics, Protvino, Russia*

<sup>d</sup>*Dipartimento di Fisica, Università di Lecce and I.N.F.N. - Sezione di Lecce, Italy*

---

## Abstract

We present results on efficiency and time resolution of a large-resistive plate chamber prototype, equipped with the final ATLAS front-end electronics, at the Gamma Irradiation Facility installed on the X5 beam of the CERN. © 2000 Elsevier Science B.V. All rights reserved.

*Keywords:* RPC; ATLAS; Front-end electronics

---

## 1. Introduction

The LHC background will be dominated by soft neutrons and gammas generated by beam protons lost at very small angle [1]. In order to cope with this background, the first-level muon trigger requires a dedicated detector of high rate capability and of high time resolution, which is essential for bunch crossing identification.

This paper describes a beam test performed on an RPC prototype at the CERN X5-GIF irradiation facility which allows to reproduce the LHC soft background by uniformly irradiating large-area detectors.

The tested RPC module is the first full-size ATLAS prototype which was equipped with gallium arsenide (GaAs) front-end electronics [2], specifically designed for the avalanche mode operation, which is the most suitable for high rates [3]. This full-custom-integrated circuit, differently from other previously utilized circuits [4], integrates in a single die both the analog and digital signal processing. It is based on a three-stage voltage amplifier connected to a comparator and is implemented in a single eight-channel layout. Output signals are ECL standard 5 ns shaped. The frequency response is peaked at 100 MHz with a 3 dB bandwidth of 160 MHz. The power consumption is less than 30 mW per channel. The front electronics in the ATLAS trigger system is installed inside the detector Faraday cage.

---

\* Corresponding author. Tel: +06-2025028; fax: +06-2023507.  
E-mail address: barbara.liberti@roma2.infn.it (B. Liberti).

## 2. Experimental lay-out

The X5 beam at SPS West Area provides muons from secondary beam pions decay. It produces some  $10^4$  muons per burst, which are contained within an area of about  $10 \times 10 \text{ cm}^2$  and an halo spread over several square metres. The muon energy was set at 100 GeV in the test. The Gamma Irradiation Facility (GIF) utilizes a  $^{137}\text{Cs}$  source of 740 GBq nominal activity, emitting a single photon of energy  $E_\gamma = 0.66 \text{ MeV}$  in 80% decays. A properly step shaped steel plug 2 mm thick is shielding the front irradiation opening, to make the photon flux uniform over large-area detectors. Several overlapping filters, moved by a remote control system, set a variable overall absorption factor which allows to modulate the photon flux intensity  $I$ , from the maximum value ( $I = 1$ ) to zero ( $I = 0$ ).

The RPC prototype under test is built according to the standard reported in Ref. [5]. It has an active area of  $176.7 \times 80.6 \text{ cm}^2$  and a two coordinate read-out, for a total of  $24 \times 56$  pick-up strips, 2.9 mm wide with 3.1 mm pitch. The data acquisition scheme is shown in Fig. 1. The front-end ECL output signals are first converted to TTL by a receiver board and then shaped at  $\sim 100 \text{ ns}$  to be sent to the control room through 40 m long flat cables. The long shaping time avoids amplitude reduction due to the cables.

In the control room, the signals are reshaped and sent to a 32 channels multihit TDC with a 16 hit buffer per channel, 1 ns Less Significant Bit (LSB)

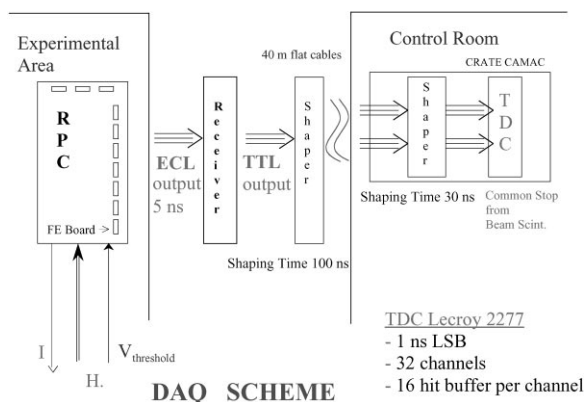


Fig. 1. DAQ schematic sketch.

and full time range of  $64 \mu\text{s}$  in common stop working mode.

Sixteen detector pick-up strips per view, defining a detector area of  $\sim 50 \times 50 \text{ cm}^2$ , are read out by the TDC.

High voltage, low voltage and the comparator threshold, are remote controlled. The total current as well as the environment variables, temperature and pressure, are monitored.

The TDC common stop signal is given by the triple coincidence of the beam scintillators S1, S2 ( $10 \times 15 \text{ cm}^2$  each) and S3 ( $10 \times 10 \text{ cm}^2$ ). The latter scintillator has air light guide to minimize spurious counting due to Cherenkov effects. The experimental layout is shown in Fig. 2. The RPC gas mixture  $\text{CH}_2\text{F}_4/\text{C}_4\text{H}_{10}/\text{SF}_6 = 96.7/3.0/0.3$  was used in the test.

## 3. Results

The time distribution of the hits acquired in the last  $10 \mu\text{s}$  before the common stop signal, provided by the muon beam trigger, is shown in Fig. 3, for full-intensity irradiation ( $I = 1$ ). The beam hits, fully contained in a single 40 ns bin, are clearly discriminated from the gammas background,

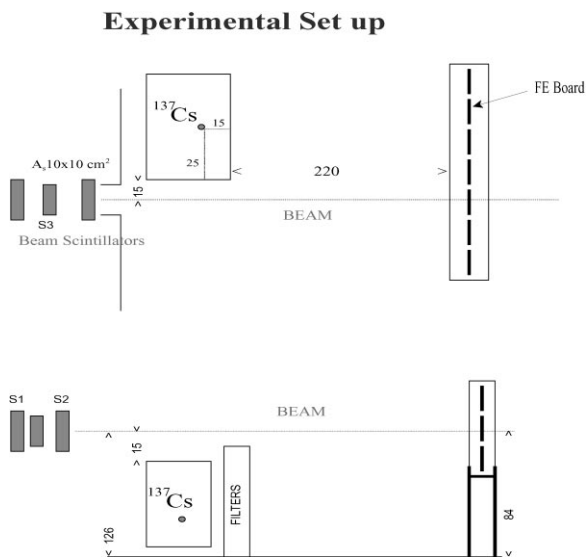


Fig. 2. Experimental layout. Top view (top) and side view (bottom). The distances are expressed in cm.

which are uniformly distributed over the full scale range.

The average arrival time of different strips are equalized off-line for taking into account systematic differences among the read-out channels.

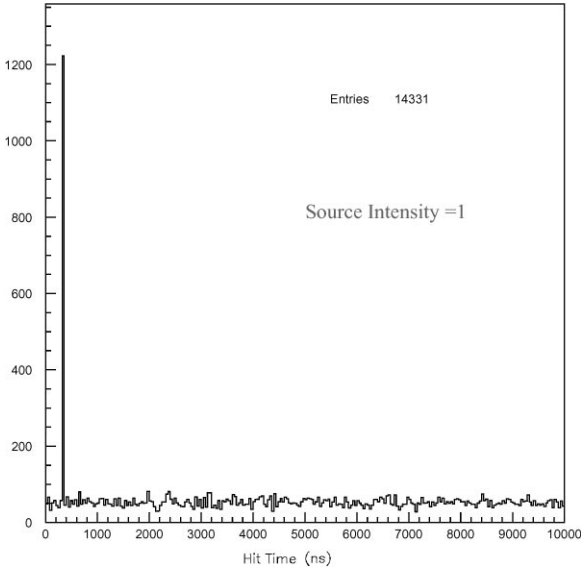


Fig. 3. Hit time distribution with open source ( $I = 1$ ) at full efficiency.

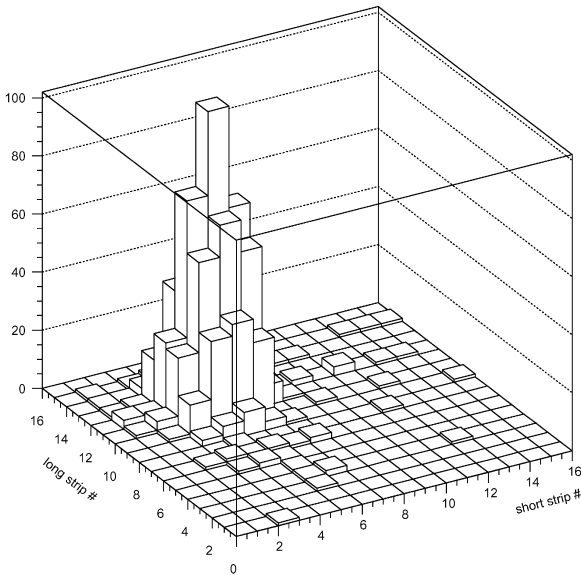


Fig. 4. Beam profile at plateau efficiency with open source ( $I = 1$ ).

The selection of trigger events for which the detector is considered efficient is performed according to the following procedure. A 10 ns acceptance window centered on the beam time peak is defined. For each trigger the hit sequences of all 16 strips in

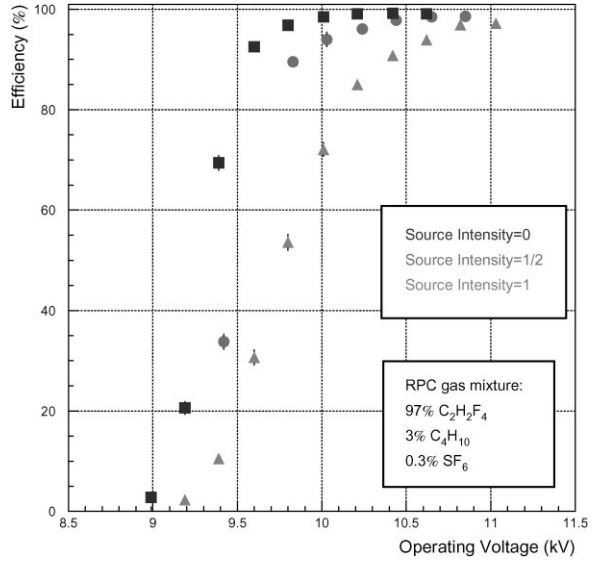


Fig. 5. Efficiency versus operating voltage at different source irradiation.

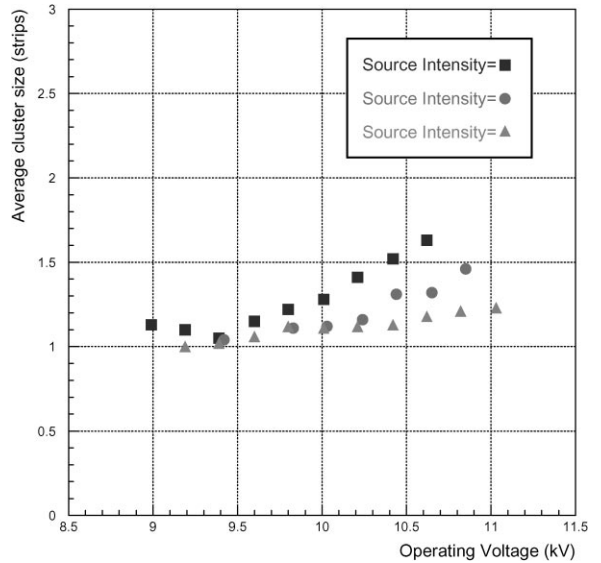


Fig. 6. Average cluster size versus operating voltage at different source irradiation.

each view are scanned and only the hits falling inside the acceptance window are selected. These hits provide the clusters pattern for each trigger.

The beam profile at full intensity source and plateau efficiency (shown in Fig. 4) is contained in a  $4 \times 4$  strips area consistent with the trigger scintillator sizes and with the beam specifications.

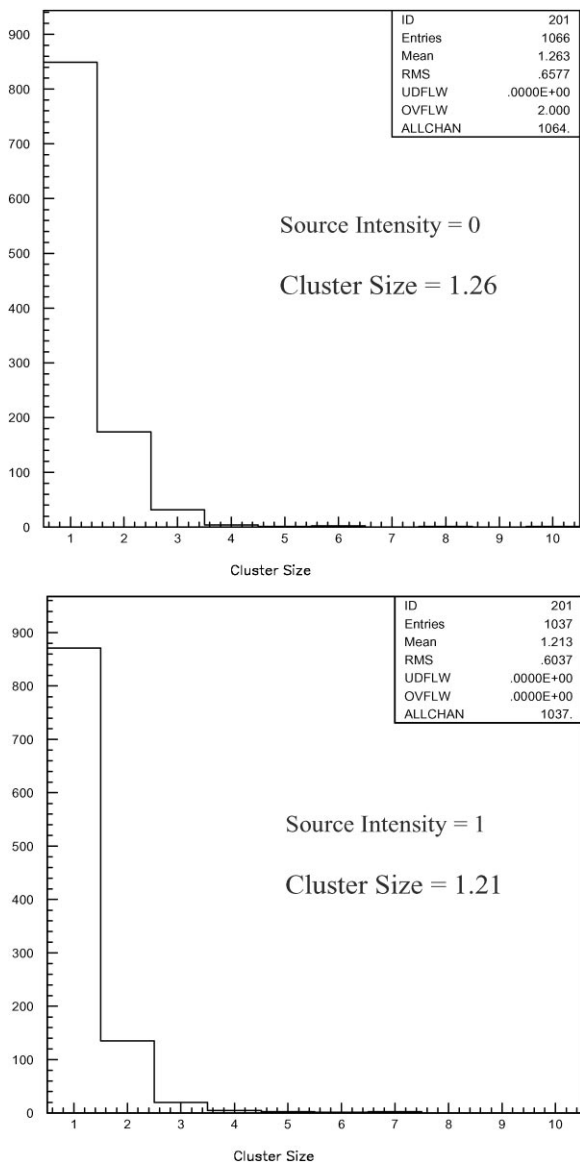


Fig. 7. Cluster distribution with closed (upper) and open (lower) source at plateau efficiency.

The detection efficiency and the average cluster size versus the operating voltage are shown in Fig. 5 and 6, respectively, at different source intensities. The cluster size distributions, at plateau efficiencies, are shown in Fig. 7

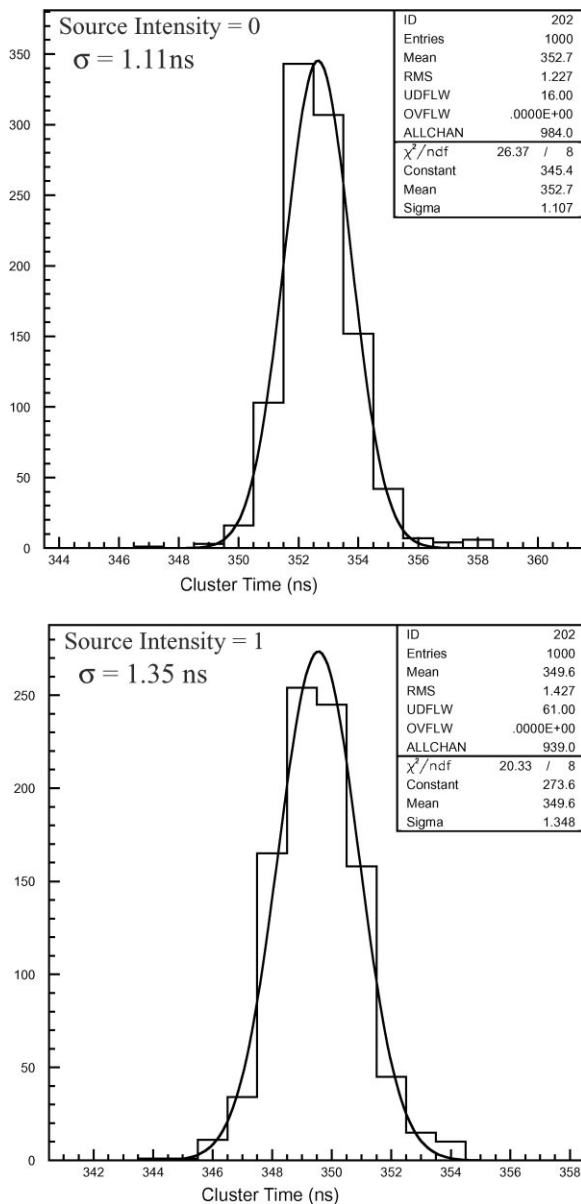


Fig. 8. Time jitter distribution at plateau efficiency with closed (upper) and open (lower) source. The operating voltages are 10.2 and 10.8 kV, respectively.

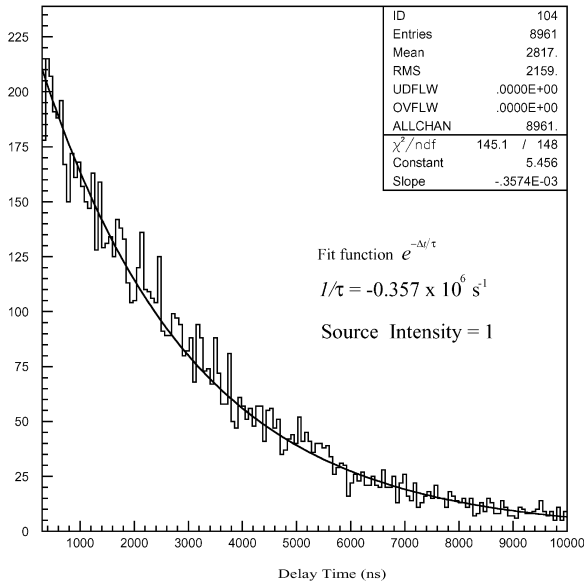


Fig. 9. Next hit delay time distribution with open source ( $I = 1$ ).

The time distributions at plateau efficiency, shown in Fig. 8, give time resolutions  $\sigma_t = 1.1$  ns and  $\sigma_t = 1.4$  ns for source on and off, respectively. For events with cluster size  $\geq 2$  the time reported in the distributions is the minimum among the cluster strips.

Fig. 9 shows the distribution of the ‘next hit delay’ for full-intensity source ( $I = 1$ ). The exponential fit  $f(t) = A \exp^{-\Delta t/\tau}$  gives  $1/\tau = (379 \pm 7) \times 10^3 \text{ s}^{-1}$  with  $\chi^2/\text{dof} = 0.98$ , indicating that the gamma detection is a stochastic process not affected by systematic effects.

Normalizing this result to the average cluster size and to the strip area, we obtain a rate per unit surface which is plotted versus the operating voltage in Fig. 10

#### 4. Conclusions

The plateau efficiency of the tested RPC prototype is  $\sim 99\%$  with source off and  $\sim 97\%$  under

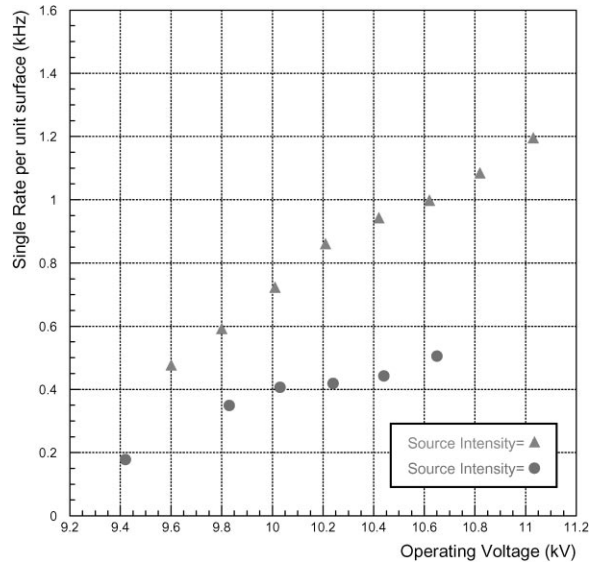


Fig. 10. Counting rate versus high voltage for  $V_{th} = 0.9$  V, with full and half irradiation intensities.

full-intensity irradiation. In the latter case, counting rate is  $\sim 1.2 \text{ kHz/cm}^2$ , about two orders of magnitude larger than the rate expected at LHC working conditions in the barrel region.

This efficiency is measured with the requirement of a total time jitter  $< \pm 5$  ns, well inside the LHC 25 ns interbunch crossing time. The cluster size at plateau efficiency remains well below two strips. The time resolution is  $\sigma_t < 1.4$  ns even at full irradiation intensity.

#### References

- [1] A. Ferrari, P. Sala, ATLAS Internal Note MUON-NO-162, 1997.
- [2] G. Aielli et al., Nucl. Instr. and Meth. A 409 (1998) 317.
- [3] M. Abbrescia et al., Nucl. Instr. and Meth. B 44 (1995) 218.
- [4] P. Camarri et al., Nucl. Instr. and Meth. A 414 (1998) 291.
- [5] The ATLAS Collaboration, ATLAS Muon Spectrometer Technical Design Report, CERN/LHCC, Vol. 97-22, 1997 p. 281.